

WRINKLE RIDGE FORMATION NORTH OF ORCUS PATERA, MARS. Matthew H. Silver¹, Andrew S. Gendaszek², Eric B. Grosfils³, Susan E. H. Sakimoto⁴, Carl V. Mendelson⁵, and Jacob E. Bleacher⁶. ¹Whitman College, Walla Walla, WA 99362 (silvermh@whitman.edu), ²Carleton College, Northfield, MN 55057, ³Pomona College, Claremont, CA 91711 (egrosfils@pomona.edu), ⁴UMBC at NASA's GSFC, Geodynamics Branch, Code 921, Greenbelt, MD 20771, ⁵Beloit College, Beloit, WI 53511, ⁶Arizona State University, Tempe, AZ 85287.

INTRODUCTION Wrinkle ridges are linear to sub-linear positive landforms produced by compression [1,2]. They are common on several planetary bodies, including Mars, Earth, Venus, the Moon, and Mercury (see discussion in [2]). On Mars they are typically found on ridged plains, which are inferred to consist of strong material such as basalt [3]. The topography of these landforms is thought to reflect their internal structure and can thus provide insight into the mechanics of formation, which has previously been interpreted as the result of a combination of faulting and folding [1-3]. Important geometric parameters of wrinkle ridges include width, height and an elevation offset of topography on either side of the ridge (Figure 1) [4].

Several mechanical models to account for wrinkle ridges have been proposed; all include faulting but vary in the depth of penetration [e.g., 2-4]. One model proposes deep fault penetration (and thus requires the absence of a décollement) and does not require systematic spacing of ridges [1,4,5]. A contrasting model predicts that faulting takes place above a décollement and is the result of processes such as gravity creep [3] or some form of lithospheric compression [e.g., 6]. Parallel, uniformly spaced ridges can be indicative of either scenario [7], but if they occur on a regional slope, gravity creep is considered to be the more likely mechanism. In this study we use data obtained from the Mars Orbiter Laser Altimeter (MOLA) to characterize the morphology of north-south trending wrinkle ridges present in the lowlands north of Orcus Patera, and then compare these geometric data to the topography predicted for each type of fault model.

METHODS Because the ridges and MOLA profiles both trend approximately north-south, we used gridded data (64 pixels/°Lon by 256 pixels/°Lat) and the program *Gridview* [8] to generate east-west topographic profiles perpendicular to the average trend of each ridge. For each profile, three geometric parameters (width, elevation offset, and height) were calculated using six data points: west-edge elevation, crest elevation, east-edge elevation, west-edge longitude, crest longitude, and east-edge longitude (Figure 1).

To discriminate between existing models, one cross-sectional wrinkle ridge profile was unfolded and measured in order to compare surface distance across the ridge after folding to the distance between the two endpoints of the ridge profile (Figure 1). For this same

profile we calculated shortened horizontal distance due to faulting using elevation offset data and an assumed minimum fault dip of 25°.

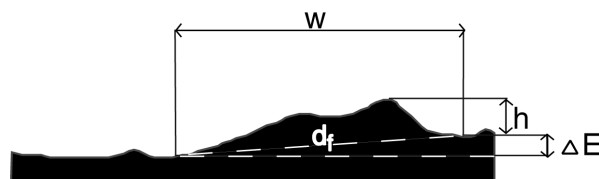


Figure 1. Wrinkle ridge dimensions: w = width, ΔE = elevation offset, h = height from crest to higher side, d_f = distance between the two endpoints of the ridge profile. V.E. $\sim 50x$.

RESULTS We constructed fourteen *Gridview* profiles, each perpendicular to one of two ridges. For each profile we calculated the ridge's width, height, and elevation offset, as defined in Figure 1. Widths range from 33 to 54 km (± 3 km) with an average of 41 km, heights range from 63 to 216 m (± 1 m) with an average of 120 m, and elevation offsets range from 2 to 48 m (± 1 m) with an average of 35 m; we find no evidence that the observed offsets are due to secondary processes (e.g., sediment deposition). Two other wrinkle ridges in our study area, located from 176.5°E to 178.5°E and from 19.5°N to 21°N, also show elevation offsets. On these two ridges, the higher side of the elevation offset is the east side for the western ridge and the west side for the eastern ridge. Ridges in our study area are irregularly spaced and occur on a regional slope dipping 0.0002° eastward from 172°E to 188°E and 0.0006° southward from 22°N to 12°N. We measured an unfolded ridge width for a typical profile in our study and from it determined a shortening due to folding (S_{fold}) value (minus distance between endpoints as defined in Figure 1) of 9.5 m. Shortening due to faulting (S_{fault}), for the same ridge, is 76 m.

DISCUSSION The topographic profiles we compiled show that wrinkle ridges in our study area are much broader than they appear in Viking images. The width of the ridges studied here is an average of 41 km with a standard deviation of 6 km. The profiles shown in [1] for wrinkle ridges in the Lunae Planum region, derived using photogrammetry, show average widths of 4.4 km with a standard deviation of 1.5 km. While we cannot directly compare the results of our study to those of [1] because different ridges were studied, lighting conditions in our study area would also lead us to infer such narrow widths in the absence of the MOLA data, and

thus it seems likely that previous measurements made using photoclinometry may underestimate ridge width.

The uniform spacing of wrinkle ridges has, in previous studies, been interpreted as the result of buckling of a plains unit at a critical wavelength [3,7]. In our region however, where the wrinkle ridges are not spaced uniformly, we infer that the wrinkle ridges did not form due to buckling at a critical wavelength. Instead, the irregularity of ridge spacing is better explained by fault-propagation and/or fault-bend folding [7].

Models previously proposed to account for typical wrinkle-ridge morphology include fault-bend and fault-propagation folding [e.g., 2]. A comparison between S_{fault} and S_{fold} is typically used to determine which is the preferred model. Should S_{fault} greatly exceed S_{fold} , a fault-bend fold is inferred because the fault must break the surface to account for this comparison of strain. Should S_{fold} be greater than or equal to S_{fault} , the fault tip dies in the subsurface and a fault-propagation fold is inferred [1,2]. Previous studies [e.g., 1,2,4,5] of wrinkle ridges have adopted standard methods of calculating S_{fault} and S_{fold} . $S_{\text{fault}}: S_{\text{fold}}$ values previously calculated are 7 [1] and 5-20 [5]. For a typical profile in our study, we calculated an $S_{\text{fault}}: S_{\text{fold}}$ value of 8. Our results, as well as those of [1,5], suggest that primary thrust faults beneath wrinkle ridges break the surface whereas smaller splay faults die in the fold and generate the "wrinkle". However, the occurrence of a simple fault-bend fold requires that width and height remain constant for a significant distance along strike and that elevation be conserved on either side of the fold [1,2,6]. From our data it is clear that elevation offsets are present and that the width and height of the ridges decrease toward each terminus. Thus, not even fault-bend folding can fully account for the surface morphology revealed in our data.

A key issue addressed by many studies of wrinkle ridges is whether a regional décollement is present. If a décollement is present and deformation is due to gravity creep of material above it, a significant regional slope is required perpendicular to the ridges. Regional ridge-perpendicular slope for our study area, however, is only 0.0002° . In addition, if gravity creep were the deforming mechanism for these north-south trending wrinkle ridges, areas such as Elysium Mons to the west and the Tharsis region to the east are likely points of creep origin due to their high gravitational potential. This makes east-higher elevation offsets on ridges coming away from Tharsis and west-higher elevation offsets on ridges coming away from Elysium Mons most likely, with a transition somewhere in between. However, our profiles for the two laterally adjacent ridges discussed earlier show a geometry opposite to that expected from gravity creep: a plateau between the

two ridges is higher than the level of the plains on the far sides of each ridge. If gravity creep is inferred this geometry can only be explained by backthrusting—not impossible but far less probable than forethrusting. Thus, the combination of the absence of a significant regional slope and the improbability of the above ridge geometry make thin-skinned deformation with gravity creep an unlikely mechanism.

The possibility exists that some thin-skinned process that is capable of acting without a regional slope produced these wrinkle ridges. However, our data do not support this possibility because the presence of a décollement is incompatible with elevation offsets and varying width and height along strike [1,2,5,6]. No known combination of folding and thrusting above a décollement can explain our basic geometric observations, so we contend that no décollement is present.

The depth of fault penetration, in the absence of a décollement, is calculated using the width of the ridge and an assumed minimum fault dip of 25° [4,5]. This model predicts, for an average ridge width, fault depth penetrations of 21 km and 17 km for the two wrinkle ridges we studied. Greater depth of penetration (25 km) is calculated for wrinkle ridges in Solis Planum [4]; these authors assume that the faults extend from one ridge to the next whereas we limit fault extent to the width of the overlying ridge. In either case, the resulting depth of penetration compares to that of some known basement thrusts on Earth [e.g., 5].

Our data show that wrinkle ridges north of Orcus Patera are wide features with gentle topography. Due to the absence of a regional slope, we find gravity creep to be an unlikely mechanism for the formation of these ridges. Other possible mechanisms include fault-propagation and fault-bend folding: a strain comparison between faulting and folding shows that the thrust faults must break the surface, thus ruling out fault-propagation folding, while the presence of elevation offsets as well as decreases in the width and height along strike lead us to believe that the ridges are not produced by fault-bend folding. We thus see deep-penetrating faults as the most plausible mechanism to account for observed wrinkle ridge morphology.

REFERENCES 1] Golombek M.P. et al. (1991) *Proc. 21st LPSC*, 679-93. 2] Schultz R.A. (2000) *JGR*, 105, 12035-52. 3] Watters T.R. (1991) *JGR*, 96, 15599-616. 4] Golombek M. et al. (2000) *LPS XXXI, abst. 1294*. 5] Golombek M. et al. (1989) *LPI Tech. Rep. 89-06*, 36-38. 6] Suppe J. & Connors C. (1992) *JGR*, 97, 13545-61. 7] Zuber M.T. & Aist L.L. (1990) *JGR*, 95, 14215-30. 8] Roark J. et al. (2000) *LPS XXXI, abst. 2026*.